



HAL
open science

Halo Structure of the Neutron-Dripline Nucleus ^{19}B

K.J. Cook, T. Nakamura, Y. Kondo, K. Hagino, K. Ogata, A.T. Saito, N.L. Achouri, T. Aumann, H. Baba, F. Delaunay, et al.

► **To cite this version:**

K.J. Cook, T. Nakamura, Y. Kondo, K. Hagino, K. Ogata, et al.. Halo Structure of the Neutron-Dripline Nucleus ^{19}B . Physical Review Letters, 2020, 124 (21), pp.212503. 10.1103/PhysRevLett.124.212503 . hal-02870791

HAL Id: hal-02870791

<https://hal.science/hal-02870791v1>

Submitted on 20 Nov 2020

HAL is a multi-disciplinary open access archive for the deposit and dissemination of scientific research documents, whether they are published or not. The documents may come from teaching and research institutions in France or abroad, or from public or private research centers.

L'archive ouverte pluridisciplinaire **HAL**, est destinée au dépôt et à la diffusion de documents scientifiques de niveau recherche, publiés ou non, émanant des établissements d'enseignement et de recherche français ou étrangers, des laboratoires publics ou privés.

The halo structure of the neutron-dripline nucleus ^{19}B

K.J. Cook,^{1,*} T. Nakamura,¹ Y. Kondo,¹ K. Hagino,² K. Ogata,^{3,4} A.T. Saito,¹ N.L. Achouri,⁵ T. Aumann,^{6,7} H. Baba,⁸ F. Delaunay,⁵ Q. Deshayes,⁵ P. Doornenbal,⁸ N. Fukuda,⁸ J. Gibelin,⁵ J.W. Hwang,⁹ N. Inabe,⁸ T. Isobe,⁸ D. Kameda,⁸ D. Kanno,¹ S. Kim,⁹ N. Kobayashi,¹ T. Kobayashi,¹⁰ T. Kubo,⁸ S. Leblond,^{5,†} J. Lee,^{8,‡} F.M. Marqués,⁵ R. Minikata,¹ T. Motobayashi,⁸ K. Muto,¹⁰ T. Murakami,² D. Murai,¹¹ T. Nakashima,¹ N. Nakatsuka,² A. Navin,¹² S. Nishi,¹ S. Ogoshi,¹ N.A. Orr,⁵ H. Otsu,⁸ H. Sato,⁸ Y. Satou,⁹ Y. Shimizu,⁸ H. Suzuki,⁸ K. Takahashi,¹⁰ H. Takeda,⁸ S. Takeuchi,⁸ R. Tanaka,¹ Y. Togano,⁷ J. Tsubota,¹ A.G. Tuff,¹³ M. Vandebrouck,^{14,§} and K. Yoneda⁸

¹*Department of Physics, Tokyo Institute of Technology,
2-12-1 O-Okayama, Meguro, Tokyo 152-8551, Japan*

²*Department of Physics, Kyoto University, Kyoto 606-8502, Japan*

³*Research Center for Nuclear Physics, Osaka University, Ibaraki 567-0047, Japan*

⁴*Department of Physics, Osaka City University, Osaka 558-8585, Japan*

⁵*LPC Caen, Normandie Université, ENSICAEN, UNICAEN, CNRS/IN2P3, Caen, France*

⁶*Institut für Kernphysik, Technische Universität Darmstadt, D-64289 Darmstadt, Germany*

⁷*ExtreMe Matter Institute EMMI and Research Division,
GSI Helmholtzzentrum für Schwerionenforschung GmbH, D-64291 Darmstadt, Germany*

⁸*RIKEN Nishina Center, Hirosawa 2-1, Wako, Saitama 351-0198, Japan*

⁹*Department of Physics and Astronomy, Seoul National University, 599 Gwanak, Seoul 151-742, Republic of Korea*

¹⁰*Department of Physics, Tohoku University, Aramaki Aoba 6-3, Aoba, Sendai, Miyagi 980-8578, Japan*

¹¹*Department of Physics, Rikkyo University, Toshima, Tokyo 171-8501, Japan*

¹²*GANIL, CEA/DRF-CNRS/IN2P3, F-14076 Caen Cedex 5, France*

¹³*Department of Physics, University of York, Heslington, York YO10 5DD, United Kingdom*

¹⁴*IPN Orsay, Université Paris Sud, IN2P3-CNRS, F-91406 Orsay Cedex, France*

The heaviest bound isotope of boron, ^{19}B , has been investigated using exclusive measurements of its Coulomb dissociation, into ^{17}B and two neutrons, in collisions with Pb at 220 MeV/nucleon. Enhanced electric dipole ($E1$) strength is observed just above the two-neutron decay threshold with an integrated $E1$ strength of $B(E1) = 1.64 \pm 0.06(\text{stat}) \pm 0.12(\text{sys}) \text{ e}^2 \text{ fm}^2$ for relative energies below 6 MeV. This feature, known as a soft $E1$ excitation, provides the first firm evidence that ^{19}B has a prominent two-neutron halo. Three-body calculations that reproduce the energy spectrum indicate that the valence neutrons have a significant s-wave configuration and exhibit a dineutron-like correlation.

Experiments at advanced radioactive beam facilities are allowing us to approach the neutron rich limit of the nuclear chart – the neutron dripline – for heavier and heavier nuclei [1, 2]. A notable feature of near-dripline nuclei is that they may exhibit neutron halos: valence neutrons that are spatially decoupled, extending far outside of the core, drastically enhancing their size. This can only occur when the valence neutron(s) are weakly bound and have low orbital angular momentum ($\ell = 0, 1$) [3]. In the conventional shell-model, halos are not expected to be a general feature of dripline nuclei owing to the limited number of low- ℓ orbitals. Conversely, if deformation develops, breaking spherical symmetry, the number of single-particle levels with low- ℓ components increase, making halos abundant at the neutron dripline [4]. Furthermore, heavier drip-line nuclei offer more opportunities to study multineutron halos comprising two or more neutrons. Such halos are particularly interesting as a possible site for the not-yet-established ‘dineutron’, a spatially compact neutron pair [5, 6]. However, detailed experimental data on multineutron halos are available only for the light classical two-neutron halos ^6He [7, 8] and ^{11}Li [9–13]. It is therefore critical to understand

the interplay among halo structures, two-neutron correlations, and shell evolution in increasingly heavy neutron-rich nuclides.

The heaviest bound isotope of boron, ^{19}B , is a candidate for detailed investigations of a possible multineutron halo. Little is known about this nuclide experimentally: it is bound with a very low (but uncertain) two neutron separation energy ($S_{2n} = 0.089_{-0.089}^{+0.560}$ MeV [14]) and has an enhanced interaction cross-section [15]. Since ^{18}B is unbound, ^{19}B is Borromean nucleus, where the three-body system is bound but none of its two-body subsystems are. These properties are suggestive of a two-neutron halo structure. However, being also weakly-bound to four neutron removal ($S_{4n} = 1.47 \pm 0.35$ MeV [16]), ^{19}B might better be described as “core plus $4n$ ” halo or as having a neutron skin [15, 17]. Previous analysis of the interaction cross-section and the two-neutron separation energies suggested that the valence neutrons in ^{19}B are predominantly d -wave, inhibiting halo formation [15, 18, 19]. The structure of ^{19}B is also relevant for the newly discovered unbound isotopes $^{20,21}\text{B}$ [20]. Intriguingly, ^{18}B , the unbound $^{17}\text{B}+n$ system, shows the largest (most negative) known scattering

length $a_s < -50$ fm of any nuclear system [21]. This extreme scattering length may be relevant to Efimov states [22–24], a general feature of three-body systems where at least two of the two-body subsystems approach infinite s -wave scattering length. Such states are of interest to atomic and molecular physics [24] but have not yet been identified in nuclei.

This Letter presents the results of the first exclusive measurement and invariant mass spectroscopy of the Coulomb dissociation of ^{19}B on a Pb target at 220 MeV/nucleon. Coulomb dissociation is an established tool to determine the electric dipole ($E1$) response of weakly bound nuclei [1, 25]. The soft $E1$ excitation, a large enhancement of the electric dipole strength at low excitation energies, is uniquely and universally seen in halo nuclides [25, 26]; resulting in an enhanced Coulomb dissociation cross-section. In $1n$ halos, the amplitude and spectral shape of the soft $E1$ excitation probes the valence neutron density distribution, providing information on the halo configuration [25–27]. The interpretation of the soft $E1$ excitation is more complex for $2n$ halos, being also sensitive to dineutron correlations and final-state interactions [25]. The $E1$ response has been measured in only three $2n$ halo nuclei: ^6He [7, 8], ^{11}Li [9–13] and ^{14}Be [28]. Beyond the intrinsic interests in ^{19}B described above, understanding how $2n$ halos evolve with increasing mass and complexity is necessary to clarify the mechanisms driving the $E1$ response in multinucleon halos. In this Letter, we extract the Coulomb dissociation energy differential cross-section and the $E1$ strength distribution, $B(E1)$. These results show that ^{19}B has a $2n$ halo. By comparing to three-body model calculations, we find agreement for $S_{2n} \sim 0.5$ MeV, a substantial s -wave component and a pronounced dineutron correlation.

The experiment was performed at the RIKEN Radioactive Ion Beam Factory (RIBF). A secondary beam containing ^{19}B (~ 120 pps) was produced by projectile fragmentation of ^{48}Ca on a Be target at 345 MeV/nucleon. The beam was isotopically identified on an event-by-event basis with the BigRIPS fragment separator [29, 30] and characterised using plastic scintillator timing detectors, an ionization chamber, and two multi-wire drift chambers (MWDCs). At the mid-point of the 3.3 g/cm 2 lead target, the average beam energy was 220 MeV/nucleon. Measurements were also made on a carbon target (1.8 g/cm 2) to evaluate the nuclear breakup component. The background produced due to reactions on materials other than the targets was characterized by measurements taken without a target, and has been subtracted in the results reported here.

The breakup products, ^{17}B and two neutrons, were detected in coincidence using SAMURAI [31]. The momentum of charged particles were reconstructed by measuring the trajectories of charged particles using two MWDCs placed before and after the large-gap superconducting dipole magnet of SAMURAI, which was kept under vac-

TABLE I. Exclusive $^{17}\text{B}+2n$ ($E_{\text{rel}} \leq 6$ MeV) and inclusive $2n$ and $4n$ removal cross-sections for reactions of ^{19}B with Pb and C targets and their ratios. The systematic error is also shown for the exclusive cross-sections.

	$\sigma_{^{17}\text{B}+2n}$ (mb)	σ_{-2n} (mb)	σ_{-4n} (mb)
$^{19}\text{B} + \text{Pb}$	1160(30)(70)	1800(60)	600(30)
$^{19}\text{B} + \text{C}$	54(3)(3)	251(5)	185(3)
$\sigma_{\text{Pb}}/\sigma_{\text{C}}$	22(1)	7.1(3)	3.3(2)

uum to minimize scattering [32]. Time-of-flight and energy loss of the charged fragments were measured in a 16-element plastic scintillator hodoscope. Neutrons were detected in coincidence ~ 11 m downstream of the target using the large acceptance plastic scintillator array NEBULA [31, 33, 34]. NEBULA consists of 120 neutron detector modules and 24 charged particle veto modules, in a two-wall configuration. The relative energy E_{rel} between ^{17}B and the two neutrons was reconstructed from their four-momenta as:

$$E_{\text{rel}} = \sqrt{\left(\sum_i E_i\right)^2 - \left|\sum_i \vec{P}_i\right|^2} - \sum_i M_i, \quad (1)$$

where (E_i, \vec{P}_i) and M_i are the four momentum of the particle i and its rest mass, respectively. The excitation energy E_x of ^{19}B is related to E_{rel} via $E_{\text{rel}} = E_x - S_{2n}$. The energy resolution was parametrized by a Gaussian distribution of width $\sigma(E_{\text{rel}}) = 0.25E_{\text{rel}}^{0.53}$ MeV.

A critical issue in multi-neutron coincidence measurements is cross-talk – multiple hits in NEBULA induced by one neutron. The comprehensive cross-talk rejection procedures employed are detailed in Ref. [33]. To detect γ -rays from excited ^{17}B fragments, the target was surrounded by the DALI2 NaI(Tl) array [35]. For both Pb and C targets, no peak was detected in the Doppler-corrected γ -ray spectrum near the 1080 ± 15 keV excited state in ^{17}B [36–38]. The upper limit of the excited state population is estimated to be 2% and 5% in dissociation reactions with the Pb and C targets, respectively.

The two-neutron detection efficiency was extracted using a detailed GEANT4 [39] simulation [33, 40] of the setup. The simulation included all NEBULA detector effects, the beam characteristics and the reconstruction of fragment momentum in SAMURAI. All analysis procedures, including the cross-talk rejection, were incorporated in the simulation. As discussed in the more critical case of ^{26}O [34], the two-neutron detection efficiency of NEBULA remains sufficient to enable reliable extraction of cross-sections down to $E_{\text{rel}} \sim 0$ MeV.

The extracted relative energy distributions for $^{19}\text{B} \rightarrow ^{17}\text{B}+2n$ in reactions with Pb and C are shown in Fig. 1. The error bars are statistical and do not include the estimated systematic error of 6%, primarily

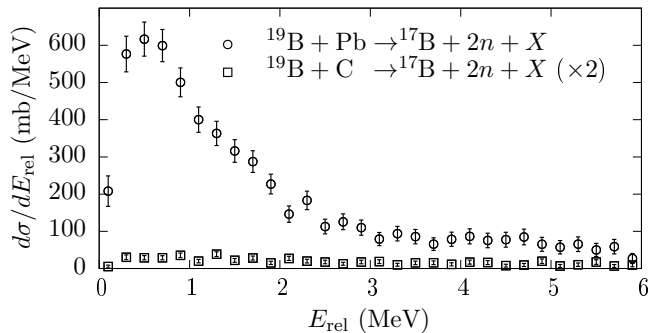


FIG. 1. Relative energy distribution of $^{19}\text{B} \rightarrow ^{17}\text{B} + 2n$ dissociation in reactions with Pb (circles) and C (squares) targets. The error bars are purely statistical.

arising from the determination of the two-neutron detection efficiency. The spectrum for the Pb target peaks at about 0.5 MeV, with a large integrated cross-section of $1160 \pm 30(\text{stat}) \pm 70(\text{sys})$ mb ($E_{\text{rel}} \leq 6$ MeV), as listed in Table I. The peak position, together with the greatly enhanced cross-section compared to C (Table I), is characteristic of the soft $E1$ excitation of a halo nucleus [25]. Quantitatively, the dissociation cross-section with the Pb target is a factor of 22(1) times larger than that for the C target, while we would only expect a factor of 2-4 for a non-halo nucleus with nearly pure nuclear dissociation [41].

The contribution of Coulomb dissociation in the $^{15}\text{B} + 4n$ channel was examined using the inclusive $2n$ and $4n$ removal cross-sections ($^{19}\text{B} \rightarrow ^{17}\text{B}$ and $^{19}\text{B} \rightarrow ^{15}\text{B}$, respectively, without neutron coincidence conditions) for reactions on Pb and C. These are shown in Table I, and account for losses of projectiles and residues arising from reactions in the targets [42] [43]. The ratio of the inclusive $-4n$ cross-sections for Pb compared to C is 3.3 ± 0.2 , consistent with the expected ratio of 2-4 for non-halo nuclei. On the other hand, the inclusive $-2n$ cross-sections have a Pb/C ratio of 7.1 ± 0.3 , reflecting the enhancement of Coulomb dissociation due to the halo in ^{19}B . Therefore, we conclude that Coulomb dissociation into $^{15}\text{B} + 4n$ is not significant and that dissociation to $^{17}\text{B} + 2n$ gives a good measure of the total Coulomb dissociation cross-section.

To deduce the Coulomb dissociation cross-section $d\sigma_{\text{CD}}/dE_{\text{rel}}$ of ^{19}B on Pb, the nuclear contribution to the total dissociation cross-section must be estimated. At 220 MeV/nucleon the grazing angle $\theta_g \sim 0.7^\circ$ (laboratory frame) is comparable to the angular resolution of the experiment ($\sigma = 0.4^\circ$, which is dominated by angular straggling ($\sigma = 0.3^\circ$) in the target). We thus chose not to select scattering angles at forward angles within θ_g as was adopted in Refs. [9, 44], but instead assume that the energy distribution of nuclear breakup is the same as the (nuclear breakup dominated) dissociation cross-section

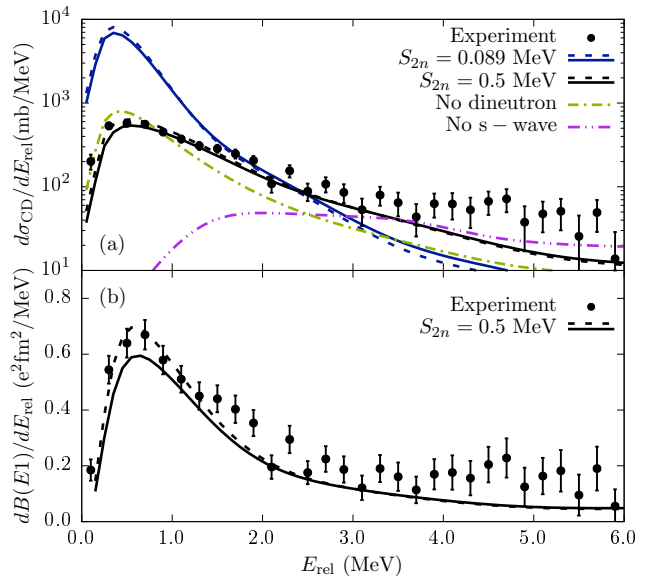


FIG. 2. (a) Coulomb dissociation cross-sections for $^{19}\text{B} \rightarrow ^{17}\text{B} + 2n$ on Pb at 220 MeV/nucleon (circles), compared to three-body model calculations at $S_{2n} = 0.089$ MeV (blue) and 0.5 MeV (black) with $a_s = -50$ fm (solid lines) and $a_s = -100$ fm (dashed lines). Dot-dot-dashed line: calculation with no s-wave contribution to the ground-state wavefunction ($S_{2n} = 0.089$ MeV, $a_s = -100$ fm). Dot-dashed line: calculation with no contribution from negative-parity orbitals ($S_{2n} = 0.3$ MeV, $a_s = -100$ fm). The experimental $B(E1)$ distribution (with $S_{2n} = 0.5$ MeV) is shown in panel (b) compared to the corresponding calculation. The error bars are statistical.

on C, multiplied by constant factor Γ , giving:

$$\frac{d\sigma_{\text{CD}}}{dE_{\text{rel}}} = \frac{d\sigma_{\text{Pb}}}{dE_{\text{rel}}} - \Gamma \frac{d\sigma_{\text{C}}}{dE_{\text{rel}}} \quad (2)$$

[45, 46]. Three-body Continuum-Discretized Coupled-Channel (CDCC) calculations of $1n$ halo nuclei have demonstrated that this method can be used to estimate σ_{CD} if Γ is about twice as large as that usually adopted from standard systematics [41]. Following Ref. [41], we estimated Γ between $S_{2n} = 0.01$ and 0.65 MeV using three-body CDCC calculations, assuming a $^{17}\text{B} + \text{dineutron}$ structure. Empirically fitting within this region, Γ depends on S_{2n} as $\Gamma = -0.9 \ln(S_{2n}) + 2.18$. The cross-section for dissociation on the C target is so small that such a change in S_{2n} results in a variation of the Coulomb dissociation cross-section of only $\sim 8\%$. Since $d\sigma_{\text{CD}}/dE_{\text{rel}}$ is weakly sensitive to Γ , we adopted $\Gamma = 2.8 \pm 1.6$ (for $S_{2n} = 0.5$ MeV, discussed later), incorporating an error arising from the S_{2n} dependence.

The resulting $d\sigma_{\text{CD}}/dE_{\text{rel}}$ is shown in Fig. 2(a). As expected from the small nuclear breakup contribution, a significant peak remains at $E_{\text{rel}} \sim 0.5$ MeV, characteristic of a halo. To interpret the Coulomb dissociation cross-section, we performed three-body ($^{17}\text{B} + n + n$) model calculations of ^{19}B with a density dependent contact pair-

ing interaction [6, 47–50], providing the $E1$ transition strength distribution $dB(E1)/dE_{\text{rel}}$. This model includes the $n-^{17}\text{B}$ and $n-n$ final-state interactions [51, 52]. A Woods-Saxon potential (radius parameter 1.27 fm, diffuseness parameter 0.7 fm) was used to describe the relative motion of $n-^{17}\text{B}$. The depth parameter was adjusted to give s-wave scattering lengths of $a_s = -50$ and -100 fm [21]. The spin-orbit potential was chosen such that a $d_{5/2}$ resonance in ^{18}B appears at $E_x = 1.1$ MeV, close to the $J^\pi = 1^-$ state predicted by shell model calculations [21] and consistent with the results obtained for single-neutron removal using the carbon target [53]. The $n-n$ interaction was adjusted to give particular S_{2n} values.

To compare to experimental data, the calculated $dB(E1)/dE_{\text{rel}}$ was transformed to $d\sigma_{\text{CD}}/dE_{\text{rel}}$ using the equivalent photon method [54]:

$$\frac{d\sigma_{\text{CD}}}{dE_{\text{rel}}} = \frac{16\pi^3}{9\hbar c} N_{E1}(E_x) \frac{dB(E1)}{dE_{\text{rel}}}. \quad (3)$$

$N_{E1}(E_x)$ is the number of $E1$ virtual photons with energy E_x exchanged in a collision, integrated between a cutoff impact parameter b_0 and infinity, where $b_0 = r_0(A_P^{1/3} + A_T^{1/3}) = 11.17$ fm, A_P , A_T are the projectile and target mass numbers, respectively, and $r_0 = 1.3$ is a radius parameter. Since S_{2n} needs to be known to map E_{rel} to excitation energy ($E_x = E_{\text{rel}} + S_{2n}$), we transformed the calculated $dB(E1)/dE_{\text{rel}}$ (with definite S_{2n}) to $d\sigma_{\text{CD}}/dE_{\text{rel}}$ for comparison to experiment. After transforming, the calculations were folded with the experimental energy resolution.

The experimental and calculated $d\sigma_{\text{CD}}/dE_{\text{rel}}$ are compared in Fig. 2(a). The solid (dashed) lines indicate a scattering length of $a_s = -50$ fm ($a_s = -100$ fm). At $E_{\text{rel}} = 0.5$ MeV, the calculations for $S_{2n} = 0.089$ MeV (blue lines) lie more than an order of magnitude above the experimental data. The model calculations for $S_{2n} = 0.5$ MeV (black lines) reproduce the experimental data significantly better. At $E_{\text{rel}} \gtrsim 3$ MeV, the calculation underestimates experiment. This is a common feature of Coulomb dissociation measurements, being seen in ^6He [7], ^{11}Be [44], ^{11}Li [9], ^{19}C [55], and can be attributed to nuclear breakup and higher order Coulomb breakup effects.

The experimental $B(E1)$ was extracted using Eq. (3) for $S_{2n} = 0.5$ MeV and is compared to calculation in Fig 2(b). Integrated up to 6 MeV, the experimental $B(E1)$ is $1.64 \pm 0.06(\text{stat}) \pm 0.12(\text{sys}) \text{ e}^2 \text{ fm}^2$. Peaking at $E_{\text{rel}} \lesssim 1$ MeV, this is the soft $E1$ excitation characteristic of a halo. Using the prescription of Ref. [49], assuming a three-body model, this $B(E1)$ corresponds to a root-mean square distance between the core and center of the two-neutron system of $\sqrt{\langle r_{c-2n}^2 \rangle} = 5.75 \pm 0.11(\text{stat}) \pm 0.21(\text{sys})$ fm. This is comparable with the estimated core- $2n$ distance of ^{11}Li , which ranges from 5.01 ± 0.32 fm [9] to 6.2 ± 0.5 fm [3].

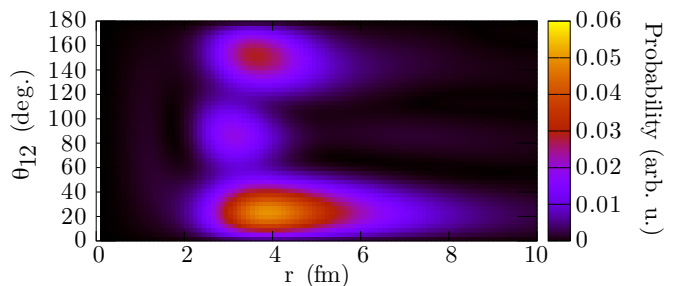


FIG. 3. Calculated [6] two-neutron probability densities for ^{19}B ($S_{2n} = 0.5$ MeV, $a_s = -50$ fm). The density (weighted by $8\pi^2 r^4 \sin \theta_{12}$) is plotted as a function of neutron-core distance, $r_1 = r_2 = r$, and opening angle between the valence neutrons θ_{12} . The density distribution shows substantial enhancement at small angles $\theta_{12} \sim 25^\circ$, indicating a dineutron correlation.

The calculation with $S_{2n} = 0.5$ MeV, $a_s = -50$ fm gives occupation probabilities of the $2s_{1/2}$, $1d_{5/2}$, and all negative parity orbitals as 35%, 56%, and 6%, respectively (the latter is dominated by contributions from fp -shell configurations). The $2s_{1/2}$ occupation probability is comparable to estimates for ^{11}Li which range from 23% [56] to 41% [57]. Our calculations assume that the valence neutrons of the inert ^{17}B core occupy only the $1d_{5/2}$ state, leaving the $2s_{1/2}$ state fully available for the valence neutrons in ^{19}B . Investigations of ^{17}B have indicated s-wave spectroscopic factors between 0.36 and 0.69 [15, 19, 58, 59]. Thus, our calculations may overestimate the $2s_{1/2}$ component in the ^{19}B halo. It is for this reason that we did not seek a best-fit value for S_{2n} . To test the extreme case of no s-wave contribution, a calculation with s-wave configurations removed from the ground-state wave-function of ^{19}B is shown by the dot-dot-dashed line in Fig. 2(a), which is clearly excluded by this experiment. We thus conclude that the valence neutrons in ^{19}B have a sizable $2s_{1/2}$ occupation, providing the low ℓ component necessary for halo formation. This is supported by investigations of ^{18}B indicating that the ground state is characterized by an s-wave virtual state with very large scattering length [21, 53]. The inclusive $-4n$ cross-section, being dominated by nuclear dissociation, also suggests that almost all of the $B(E1)$ strength is associated with $^{17}\text{B}+2n$.

The calculated two-neutron density distribution for ^{19}B ($S_{2n} = 0.5$ MeV, $a_s = -50$ fm) is shown in Fig. 3. The asymmetry in θ_{12} , concentrated at $\theta_{12} \sim 25^\circ$, indicates a strong dineutron correlation in ^{19}B . Without a dineutron correlation, the three peaked structure arising from the $(\nu d_{5/2})^2$ configuration would be symmetric about 90° [60]. The prominent asymmetry arises from the pairing interaction mixing single particle levels with opposite parities [60], making the $\sim 6\%$ admixture of negative parity valence neutron configurations crucial for the formation of a dineutron correlation in ^{19}B .

The dineutron correlation is visible in $d\sigma_{\text{CD}}/dE_{\text{rel}}$.

Calculations with contribution of the negative parity configurations artificially removed from the ground-state (removing dineutron correlation) result in a decrease in $B(E1)$ by a factor of 2 for a given S_{2n} . A calculation with no dineutron correlation with lower $S_{2n} = 0.3$ MeV ($a_s = -100$ fm), shown by the dot-dashed line in Fig. 2(a) fails to reproduce $d\sigma_{CD}/dE_{\text{rel}}$ for $E_{\text{rel}} \gtrsim 1$ MeV. While S_{2n} is uncertain, Coulomb dissociation still provides useful insight into dineutron correlations.

In summary, ^{19}B dissociation into $^{17}\text{B}+2n$ in reactions with Pb and C at 220 MeV/nucleon proves that ^{19}B has a pronounced two-neutron halo. The 22(1)-fold increase in cross-section located at small E_{rel} for reactions on Pb compared to C shows the presence of a soft $E1$ excitation in ^{19}B , a ‘fingerprint’ of a halo nucleus. The Coulomb dissociation energy spectrum compared to three-body model calculations shows good agreement for $S_{2n} \sim 0.5$ MeV. Adopting $S_{2n} = 0.5$ MeV, the electric dipole transition strength is $B(E1) = 1.64 \pm 0.06(\text{stat}) \pm 0.12(\text{sys}) e^2 \text{fm}^2$ for $E_{\text{rel}} \leq 6$ MeV, nearly equivalent to that of the established halo systems ^{11}Li [9] and ^{11}Be [45]. This largely disagrees with previous investigations that suggested a near total dominance of the $(\nu d_{5/2})^2$ configuration and a suppressed halo [15, 18]. This is likely due to the simplified two body treatment in the previous studies and the static density distribution used to derive the ^{19}B matter radius [61]. This highlights the importance of Coulomb dissociation as a tool for identifying halo structures.

Alongside our Coulomb dissociation data, a higher precision S_{2n} value is needed to fully constrain $B(E1)$. With a more precise S_{2n} , the $dB(E1)/dE_{\text{rel}}$ distribution could be used to extract information on the $^{17}\text{B}+n$ scattering length and to constrain structure models. We also note that ^{19}B is likely more complicated than a three-body system. ^{17}B is itself a Borromean $2n$ halo nucleus with a large probability of ^{15}B core excitation [37], making ^{19}B something like a *Matryoshka* doll of Borromean halo structures. Further, $^{17,19}\text{B}$ may be deformed and have a two-center cluster structure [17, 62–64]. The complexity of ^{19}B makes understanding its reactions and structure pertinent to our efforts to understand increasingly heavy drip-line systems where many-body weakly-bound nuclei may be common.

We thank the accelerator staff of the RIKEN Nishina Center for their efforts in delivering the intense ^{48}Ca beam. K.J.C. acknowledges the JSPS International Research Fellowship program at the Tokyo Institute of Technology. A.N. acknowledges the JSPS Invitation fellowship program for long term research in Japan at the Tokyo Institute of Technology. N.L.A., F.D., J.G., F.M.M., and N.A.O. acknowledge partial support from the Franco-Japanese LIA-International Associated Laboratory for Nuclear Structure Problems as well as the French ANR-14-CE33-0022-02 EXPAND. The present work was supported in part by JSPS KAKENHI Grants No. 24740154, 16H02179 and JP16K05352, MEXT

KAKENHI Grants No. 24105005 and 18H05404, the WCU (R32-2008-000-10155-0) and the GPF (NRF-2011-0006492) programs of NRF Korea, and the HIC for FAIR.

-
- * cookk@frib.msu.edu; Present Address: Facility for Rare Isotope Beams, Michigan State University, East Lansing, MI 48824, USA
 - † Present address: GANIL, CEA/DRF-CNRS/IN2P3, F-14076 Caen Cedex 5, France
 - ‡ Present address: Department of Physics, University of Hong Kong, Pokfulam Road, Hong Kong.
 - § Present address: IRFU, CEA, Université Paris-Saclay, F-91191 Gif-sur-Yvette, France
- [1] T. Nakamura, H. Sakurai, and H. Watanabe, *Prog. Part. Nucl. Phys.* **97**, 53 (2017).
 - [2] D. S. Ahn, N. Fukuda, H. Geissel, N. Inabe, N. Iwasa, T. Kubo, K. Kusaka, D. J. Morrissey, D. Murai, T. Nakamura, *et al.*, *Phys. Rev. Lett.* **123**, 212501 (2019).
 - [3] I. Tanihata, H. Savajols, and R. Kanungo, *Prog. Part. Nucl. Phys.* **68**, 215 (2013).
 - [4] I. Hamamoto, *Phys. Rev. C* **95**, 044325 (2017).
 - [5] A. Migdal, *Sov. J. Nucl. Phys* **16**, 238 (1973).
 - [6] K. Hagino and H. Sagawa, *Phys. Rev. C* **72**, 044321 (2005).
 - [7] T. Aumann, D. Aleksandrov, L. Axelsson, T. Baumann, M. J. G. Borge, L. V. Chulkov, J. Cub, W. Dostal, B. Eberlein, T. W. Elze, H. Emling, *et al.*, *Phys. Rev. C* **59**, 1252 (1999).
 - [8] J. Wang, A. Galonsky, J. J. Kruse, E. Tryggestad, R. H. White-Stevens, P. D. Zecher, Y. Iwata, K. Ieki, A. Horváth, F. Deák, *et al.*, *Phys. Rev. C* **65**, 034306 (2002).
 - [9] T. Nakamura, A. M. Vinodkumar, T. Sugimoto, N. Aoi, H. Baba, D. Bazin, N. Fukuda, T. Gomi, H. Hasegawa, N. Imai, *et al.*, *Phys. Rev. Lett.* **96**, 252502 (2006).
 - [10] K. Ieki, D. Sackett, A. Galonsky, C. A. Bertulani, J. J. Kruse, W. G. Lynch, D. J. Morrissey, N. A. Orr, H. Schulz, B. M. Sherrill, *et al.*, *Phys. Rev. Lett.* **70**, 730 (1993).
 - [11] D. Sackett, K. Ieki, A. Galonsky, C. A. Bertulani, H. Esbensen, J. J. Kruse, W. G. Lynch, D. J. Morrissey, N. A. Orr, B. M. Sherrill, *et al.*, *Phys. Rev. C* **48**, 118 (1993).
 - [12] S. Shimoura, T. Nakamura, M. Ishihara, N. Inabe, T. Kobayashi, T. Kubo, R. Siemssen, I. Tanihata, and Y. Watanabe, *Phys. Lett. B* **348**, 29 (1995).
 - [13] M. Zinser, F. Humbert, T. Nilsson, W. Schwab, H. Simon, T. Aumann, M. Borge, L. Chulkov, J. Cub, T. Elze, *et al.*, *Nucl. Phys. A* **619**, 151 (1997).
 - [14] A direct mass measurement gave $S_{2n} = 0.14_{-0.14}^{+0.39}$ MeV[18]. The present value is taken from the AME2016 compilation [16].
 - [15] T. Suzuki, R. Kanungo, O. Bochkarev, L. Chulkov, D. Cortina, M. Fukuda, H. Geissel, M. Hellström, M. Ivanov, R. Janik, *et al.*, *Nucl. Phys. A* **658**, 313 (1999).
 - [16] M. Wang, G. Audi, F. G. Kondev, W. Huang, S. Naimi, and X. Xu, *Chinese Phys. C* **41**, 030003 (2017).
 - [17] Y. Kanada-En’yo and H. Horiuchi, *Prog. Theor. Phys. Supp.* **142**, 205 (2001).
 - [18] L. Gaudefroy, W. Mittig, N. A. Orr, S. Varet,

- M. Chartier, P. Roussel-Chomaz, J. P. Ebran, B. Fernández-Domínguez, G. Frémont, P. Gangnant, *et al.*, Phys. Rev. Lett. **109**, 202503 (2012).
- [19] H. T. Fortune and R. Sherr, Eur. Phys. J. A **48**, 2 (2012).
- [20] S. Leblond, F. M. Marqués, J. Gibelin, N. A. Orr, Y. Kondo, T. Nakamura, J. Bonnard, N. Michel, N. L. Achouri, T. Aumann, *et al.*, Phys. Rev. Lett. **121**, 262502 (2018).
- [21] A. Spyrou, T. Baumann, D. Bazin, G. Blanchon, A. Bonaccorso, E. Breitbach, J. Brown, G. Christian, A. Deline, P. A. DeYoung, *et al.*, Phys. Lett. B **683**, 129 (2010).
- [22] E. Hiyama, R. Lazauskas, F. M. Marqués, and J. Carbonell, Phys. Rev. C **100**, 011603(R) (2019).
- [23] I. Mazumdar, V. Arora, and V. S. Bhasin, Phys. Rev. C **61**, 051303(R) (2000).
- [24] P. Naidon and S. Endo, Rep. Prog. Phys. **80**, 056001 (2017).
- [25] T. Aumann and T. Nakamura, Phys. Scripta **T152**, 014012 (2013).
- [26] T. Nakamura and Y. Kondo, in *Clusters in Nuclei Vol. 2, Lecture Notes in Physics*, edited by C. Beck (Springer-Verlag, Berlin Heidelberg, 2004) Chap. 2, pp. 67–119.
- [27] G. Goldstein, D. Baye, and P. Capel, Phys. Rev. C **73**, 024602 (2006).
- [28] M. Labiche, N. A. Orr, F. M. Marqués, J. C. Angélique, L. Axelsson, B. Benoit, U. C. Bergmann, M. J. G. Borge, W. N. Catford, S. P. G. Chappell, *et al.*, Phys. Rev. Lett. **86**, 600 (2001).
- [29] T. Kubo, Nucl. Instrum. Methods Phys. Res. B **204**, 97 (2003).
- [30] T. Ohnishi, T. Kubo, K. Kusaka, A. Yoshida, K. Yoshida, M. Ohtake, N. Fukuda, H. Takeda, D. Kameda, K. Tanaka, *et al.*, J. Phys. Soc. Jpn **79**, 073201 (2010).
- [31] T. Kobayashi, N. Chiga, T. Isobe, Y. Kondo, T. Kubo, K. Kusaka, T. Motobayashi, T. Nakamura, J. Ohnishi, H. Okuno, *et al.*, Nucl. Instrum. Methods Phys. Res. B **317**, 294 (2013).
- [32] Y. Shimizu, H. Otsu, T. Kobayashi, T. Kubo, T. Motobayashi, H. Sato, and K. Yoneda, Nucl. Instrum. Methods Phys. Res. B **317**, 739 (2013).
- [33] T. Nakamura and Y. Kondo, Nucl. Instrum. Methods Phys. Res. B **376**, 156 (2016).
- [34] Y. Kondo, T. Nakamura, R. Tanaka, R. Minakata, S. Ogoshi, N. A. Orr, N. L. Achouri, T. Aumann, H. Baba, F. Delaunay, *et al.*, Phys. Rev. Lett. **116**, 102503 (2016).
- [35] S. Takeuchi, T. Motobayashi, Y. Togano, M. Matsushita, N. Aoi, K. Demichi, H. Hasegawa, and H. Murakami, Nucl. Instrum. Methods Phys. Res. A **763**, 596 (2014).
- [36] Y. Kondo, T. Nakamura, N. Aoi, H. Baba, D. Bazin, N. Fukuda, T. Gomi, H. Hasegawa, N. Imai, M. Ishihara, *et al.*, Phys. Rev. C **71**, 044611 (2005).
- [37] R. Kanungo, Z. Elekes, H. Baba, Z. Dombrádi, Z. Fülöp, J. Gibelin, Á. Horváth, Y. Ichikawa, E. Ideguchi, N. Iwasa, *et al.*, Phys. Lett. B **608**, 206 (2005).
- [38] Z. Dombrádi, Z. Elekes, R. Kanungo, H. Baba, Z. Fülöp, J. Gibelin, Á. Horváth, E. Ideguchi, Y. Ichikawa, N. Iwasa, *et al.*, Phys. Lett. B **621**, 81 (2005).
- [39] S. Agostinelli, J. Allison, K. Amako, J. Apostolakis, H. Araujo, P. Arce, M. Asai, D. Axen, S. Banerjee, G. Barrand, *et al.*, Nucl. Instrum. Methods Phys. Res. A **506**, 250 (2003).
- [40] Y. Kondo, T. Tomai, and T. Nakamura, Nucl. Instrum. Methods Phys. Res. B, In Press (2019).
- [41] K. Yoshida, T. Fukui, K. Minomo, and K. Ogata, Prog. Theor. Exp. Phys. **2014**, 053D03 (2014).
- [42] N. Kobayashi, T. Nakamura, J. A. Tostevin, Y. Kondo, N. Aoi, H. Baba, S. Deguchi, J. Gibelin, M. Ishihara, Y. Kawada, *et al.*, Phys. Rev. C **86**, 054604 (2012).
- [43] Reaction cross-sections for $^{17,19}\text{B}+\text{C,Pb}$ were determined and will be presented in a future publication. Reaction cross-sections for $^{15}\text{B}+\text{C,Pb}$ were obtained with a microscopic double-folding model [65–67]. Varying the ^{15}B reaction cross-section by 10% gives a $< 1\%$ change in σ_{-4n} .
- [44] N. Fukuda, T. Nakamura, N. Aoi, N. Imai, M. Ishihara, T. Kobayashi, H. Iwasaki, T. Kubo, A. Mengoni, M. Notani, *et al.*, Phys. Rev. C **70**, 054606 (2004).
- [45] T. Nakamura, S. Shimoura, T. Kobayashi, T. Teranishi, K. Abe, N. Aoi, Y. Doki, M. Fujimaki, N. Inabe, N. Iwasa, *et al.*, Phys. Lett. B **331**, 296 (1994).
- [46] R. Palit, P. Adrich, T. Aumann, K. Boretzky, B. V. Carlson, D. Cortina, U. Datta Pramanik, T. W. Elze, H. Emling, H. Geissel, *et al.*, Phys. Rev. C **68**, 034318 (2003).
- [47] G. Bertsch and H. Esbensen, Ann. Physics **209**, 327 (1991).
- [48] H. Esbensen, G. F. Bertsch, and K. Hencken, Phys. Rev. C **56**, 3054 (1997).
- [49] H. Esbensen, K. Hagino, P. Mueller, and H. Sagawa, Phys. Rev. C **76**, 024302 (2007).
- [50] K. Hagino, H. Sagawa, J. Carbonell, and P. Schuck, Phys. Rev. Lett. **99**, 022506 (2007).
- [51] H. Esbensen and G. F. Bertsch, Nuclear Physics, Section A **542**, 310 (1992).
- [52] K. Hagino, H. Sagawa, T. Nakamura, and S. Shimoura, Phys. Rev. C **80**, 031301(R) (2009).
- [53] S. Leblond, *Structure des isotopes de bore et de carbone riches en neutrons aux limites de la stabilité*, Ph.D. thesis, Université de Caen Normandie (2015), avail: <https://tel.archives-ouvertes.fr/tel-01289381>.
- [54] C. A. Bertulani and G. Baur, Phys. Rep. **163**, 299 (1988).
- [55] T. Nakamura, N. Fukuda, T. Kobayashi, N. Aoi, H. Iwasaki, T. Kubo, A. Mengoni, M. Notani, H. Otsu, H. Sakurai, *et al.*, Phys. Rev. Lett. **83**, 1112 (1999).
- [56] H. Sagawa and K. Hagino, Eur. Phys. J. A **51**, 102 (2015).
- [57] H. Simon, M. Meister, T. Aumann, M. Borge, *et al.*, Nuclear Physics A **791**, 267 (2007).
- [58] T. Suzuki, Y. Ogawa, M. Chiba, M. Fukuda, N. Iwasa, T. Izumikawa, R. Kanungo, Y. Kawamura, A. Ozawa, T. Suda, *et al.*, Phys. Rev. Lett. **89**, 012501 (2002).
- [59] Y. Yamaguchi, C. Wu, T. Suzuki, A. Ozawa, D. Q. Fang, M. Fukuda, N. Iwasa, T. Izumikawa, H. Jeppesen, R. Kanungo, *et al.*, Phys. Rev. C **70**, 054320 (2004).
- [60] T. Oishi, K. Hagino, and H. Sagawa, Phys. Rev. C **82**, 024315 (2010).
- [61] J. S. Al-Khalili and J. A. Tostevin, Phys. Rev. Lett. **76**, 3903 (1996).
- [62] H. Takemoto, H. Horiuchi, and A. Ono, Prog. Theor. Phys. **101**, 101 (1999).
- [63] Y. Kanada-En'yo and H. Horiuchi, Phys. Rev. C **52**, 647 (1995).
- [64] G. A. Lalazissis, D. Vretenar, and P. Ring, Eur. Phys. J. A **22**, 37 (2004).
- [65] K. Minomo, K. Washiyama, and K. Ogata, (2017), arXiv:1712.10121 [nucl-th].
- [66] K. Amos, P. Dortmans, H. von Geramb, S. Karataglidis,

and J. Raynal, in *Advances in Nuclear Physics Vol 25*, Vol. 25, edited by Negele, JW and Vogt, E (Springer US, New York, 2000) pp. 275–536.

[67] K. Minomo, K. Ogata, M. Kohno, Y. R. Shimizu, and M. Yahiro, *J. Phys. G* **37**, 085011 (2010).